ADVANCED FUNCTIONAL MATERIALS
www.afm-journal.de

Design of Topology-Controlled Polyethers toward Robust Cooperative Hydrogen Bonding

Junhee Kim, Soonyoung Choi, Jinsu Baek, Yong Il Park, Jin Chul Kim, Ji-Eun Jeong, Hyocheol Jung, Tae-Hyuk Kwon, Byeong-Su Kim,* and Sang-Ho Lee**

Topology control of polymers is critical for determining their physical properties and potential applications; in particular, topologies that incorporate numerous hydrogen bonding (H-bonding) donors and acceptors along the polymer chains considerably influence the formation of different inter- and intramolecular H-bonding motifs. In this study, the high-level control of inter- and intramolecular H-bonding is investigated in topology-controlled poly(glycidoxy carbonyl benzoic acid)s (PGCs). Three types of topology-controlled PGCs (i.e., linear, hyperbranched, and branched cyclic structures having a similar degree of polymerization) are prepared by introducing aromatic carboxylic acids into the corresponding polyglycidols (PGs) via quantitative post-polymerization modification with phthalic anhydride. The obtained three types of PGCs demonstrated the high-level interplay between the inter- and intramolecular H-bonding in polymer chains by exhibiting the pH-dependent self-association properties in the solution state and the strong adhesion properties in the bulk state with high transparency. Interestingly, the dramatically enhanced adhesive property by 2.6-fold is demonstrated by simple mixing of branched cyclic PGC and topology-controlled PGs to promote the cooperative H-bonding between polymer chains. The new class of cooperative H-bonding is anticipated between topology-controlled polymers to contribute to the development of advanced adhesive and the high potential in biological and biomedical applications due to its excellent biocompatibility.

1. Introduction

In recent decades, the control of polymer topologies has attracted considerable attention in developing unique functions in artificial macromolecules as an important molecular parameter to determine their physical properties and applications.[1,2] As a unique polymer topology, dendrimers and hyperbranched polymers have been explored because of their unique physical properties, which arise from their branched multifunctional structures.[3–8] Particularly, hyperbranched polymers have received much industrial interest because of their relatively simple synthetic approach compared to dendrimers and improved physical properties compared to linear counterparts such as excellent solubility, low solution viscosity, and modified rheological properties resulting from highly branched structure. Meanwhile, as another notable type of polymer architecture, macrocyclic polymers have been investigated recently because of their lower conformational degree of freedom and more compact coil conformation compared to those of their linear analogs due to the absence of polymeric chain ends.[9–11] Although a significant effort has been demonstrated in the use of topology-controlled polymers for a wide range of applications including medicine, nanotechnology, and material science, the investigation of interactions between topology-controlled polymers is still highly desired.

Hydrogen bonding (H-bonding) is unique in nature owing to its high directionality, specificity, dynamics, and cooperativity.[12–17] For example, an array of multiple precisely placed H-bonds enables stronger specific interactions, as represented by the double helix of complementary base pairs in DNA. In addition, the application of external stimuli on the DNA strand can trigger the dissociation or association of H-bonds, which is key for several biological processes such as transcription. Inspired by these selective yet dynamic interactions in nature, efforts have been directed to the design and synthesis of novel functional materials, particularly, self-assembled supramolecules, polymer blends, copolymers, and nanocomposites.[18–22] Furthermore, H-bonding plays an important role in determining the physical, chemical, thermal, and mechanical properties of polymeric materials. For example, intermolecular

J. Kim, S. Choi, Y. I. Park, J. C. Kim, J.-E. Jeong, H. Jung, S.-H. Lee
Center for Advanced Specialty Chemicals
Korea Research Institute of Chemical Technology
Ulsan 44412, Republic of Korea
E-mail: slee@krict.re.kr
J. Kim, T.-H. Kwon
Department of Chemistry
Ulsan National Institute of Science and Technology (UNIST)
Ulsan 44919, Republic of Korea
E-mail: kwon90@unist.ac.kr
J. Baek, B.-S. Kim
Department of Chemistry
Yonsei University
Seoul 03722, Republic of Korea
E-mail: bskim19@yonsei.ac.kr
S.-H. Lee
Advanced Materials and Chemical Engineering
University of Science and Technology (UST)
Daejeon 34113, Republic of Korea

The ORCID identification number(s) for the author(s) of this article can be found under https://doi.org/10.1002/adfm.202302086.

DOI: 10.1002/adfm.202302086

H-bonding in polyamides and polyurethanes induces the formation of crystalline structures, thus leading to improved thermal and mechanical performance.[23] Multiple studies have been conducted to investigate the synthesis of polymers designed to exploit these interactions. For example, we have recently presented the poly(glycidoxy acetic acid) (PGA), carrying an H-bonding donor and acceptor within a single repeating unit of linear polymer backbone to precisely control the H-bonding in polymer chains leading to strong adhesive properties in the bulk state.[24] Additionally, Wilker et al. demonstrated a biomimetic adhesive polymer, poly(catechol-acrylic acid), that incorporates multifunctional organic alcohol groups functioning as physical crosslinkers via H-bonding to enhance the toughness and adhesive performance of the polymer.[25] Furthermore, Choi et al. demonstrated a series of well-defined polysulfonamides with single-fluorophore emitting white light via excited-state intramolecular proton transfer and precise control of the thermodynamics of the corresponding process by fine-tuning the strength of the intramolecular H-bonding.[26] Despite the successful tuning of polymer properties via H-bonding between polymer chains, most of these investigations were limited to linear polymer systems; thus, we aim to seek further tuning of the H-bonding via precise control of polymeric topology.

To approach this idea, a metal-free ring-opening polymerization of glycidol using frustrated Lewis pairs is initially employed to synthesize the hyperbranched polyglycidols (*hb*-PGs) and branched cyclic PGs (*bc*-PGs) along with the linear PGs (*lin*-PGs) control.[27,28] On the basis of these topology-controlled PGs, we envision that the quantitative post-polymerization modification of PGs would produce topology-controlled poly(glycidoxycarbonyl benzoic acid) (PGCs) having carboxylic acid pendants (H-bonding donor) within the framework of polyether (H-bonding acceptor) (**Scheme 1**). Tunable pH-dependent self-association in solution, as well as adhesive performance, were observed that are highly dictated by the PGCs through inter- and intramolecular H-bonding depending on the polymer topologies. Furthermore, a simple mixture of topology-controlled PGCs and PGs could additionally promote cooperative H-bonding between polymer chains, which leads to versatile engineering of physical properties for advanced material applications. Finally, the PGCs were tested for their biocompatibility with living cells. Considering its excellent biocompatibility, we anticipate the potential applications of PGC in biological and biomedical fields.

2. Results and Discussion

2.1. Optimization of the Post-Polymerization Modification of Topology-Controlled PGs

In order to investigate the H-bonding effect of carboxylic acid in the pendants and oxygen atom in the polyether backbone depending on the polymer topologies, we aimed to quantitatively convert the hydroxyl moiety on various PG topologies into aromatic carboxylic acid groups. To achieve this with *bc*-PG, phthalic anhydride was used for post-polymerization modification. While the functionalization of *bc*-PG with 2 equivalents of phthalic anhydride at 120 °C overnight led to a marginal degree of modification, the use of DBU as a nucleophilic catalyst for the acylation of *bc*-PG resulted in quantitative post-polymerization modification. In addition, heterogeneous PG solution in organic solvents such as toluene, dichloromethane, tetrahydrofuran, ethyl acetate, acetone, and acetonitrile became a homogeneous clear solution (Table S1 and Figure S1, Supporting Information). It is attributed to the decreased polarity of PGs by H-bonding between the hydroxyl group and DBU, as confirmed by ^{1}H NMR spectra (Figure S2, Supporting Information).

Interestingly, the acylation reaction was completed within 30 min in acetonitrile after the addition of phthalic anhydride in the mixture at room temperature, resulting in a nearly complete conversion of the hydroxyl groups in *bc*-PG (**Figure 1**a). This acceleration may occur via the formation of an active intermediate between phthalic anhydride and excess DBU in the reaction mixture, as confirmed by^{1}H NMR spectroscopy (Figure S3, Supporting Information).[30,31] Based on these results, we propose a possible acylation mechanism for the modification of PGs (Scheme S1, Supporting Information). In this mechanism, DBU, as a nucleophilic catalyst, attacks the carbonyl carbon of the phthalic anhydride to generate an active intermediate. The electron lone pair on a pendant hydroxyl group on the PG backbone then attacks the carbonyl group of the active intermediate. The reaction is then terminated by the addition of a proton source to the carboxyl group.

2.2. Structure Analyses of the Topology-Controlled PGCs

After the successful DBU-catalyzed post-polymerization modification of the synthesized PG topologies ($DP_{n,bc\text{-PG}}$ = 37, $DP_{n,hb\text{-PG}}$ = 38, and $DP_{n,lin\text{-PG}}$ = 35), the resulting topology-controlled PGCs were analyzed by ^{1}H NMR, FT-IR, SEC, and TGA to evaluate the composition of the pendant aromatic carboxylic acid groups in the polymer backbone (Figure 1; Figures S4 and S5, Supporting Information). For example, the ^{1}H NMR peaks derived from the pendant aromatic carboxylic acids in *bc*-PGC are clearly observed, including those for the polyether backbone (*a″-c″*,' 3.38–3.95 ppm), aromatic (*d″-g″*, 7.32–7.80 ppm), and carboxylic acid protons (*h*', 13.00–13.50 ppm) (Figure 1a). Peak integration of the aromatic protons indicates a quantitative conversion of >99% of the PG hydroxyls to aromatic carboxylic acids. In addition, the obtained SEC curves show UV absorptions at 270 nm that overlap with the RI signal, thus indicating the successful introduction of the aromatic groups into the polymer chain (Figure 1b). Changes in the functional moieties of the polymers are also observed in the obtained FT-IR spectra. For example, the characteristic peak of the alcohol group of *bc*-PG (3400 cm^{-1}) exhibits a reduced area after post-polymerization modification, accompanied by the appearance of peaks at 3000, 1700, 1600, and 1215 cm^{-1} attributable to acidic, carbonyl, aromatic, and ester groups, respectively (Figures S6–S8, Supporting Information). Finally, TGA analysis was conducted to quantitatively estimate the number of aromatic carboxylic acids introduced into the polymer backbone. All samples show an initial decomposition at 165 °C accompanied by a loss of ≈67 wt.%, after which a second loss of 33 wt.% is observed at 330 °C. This two-stage decomposition process indicates that the aromatic carboxylic acid groups were

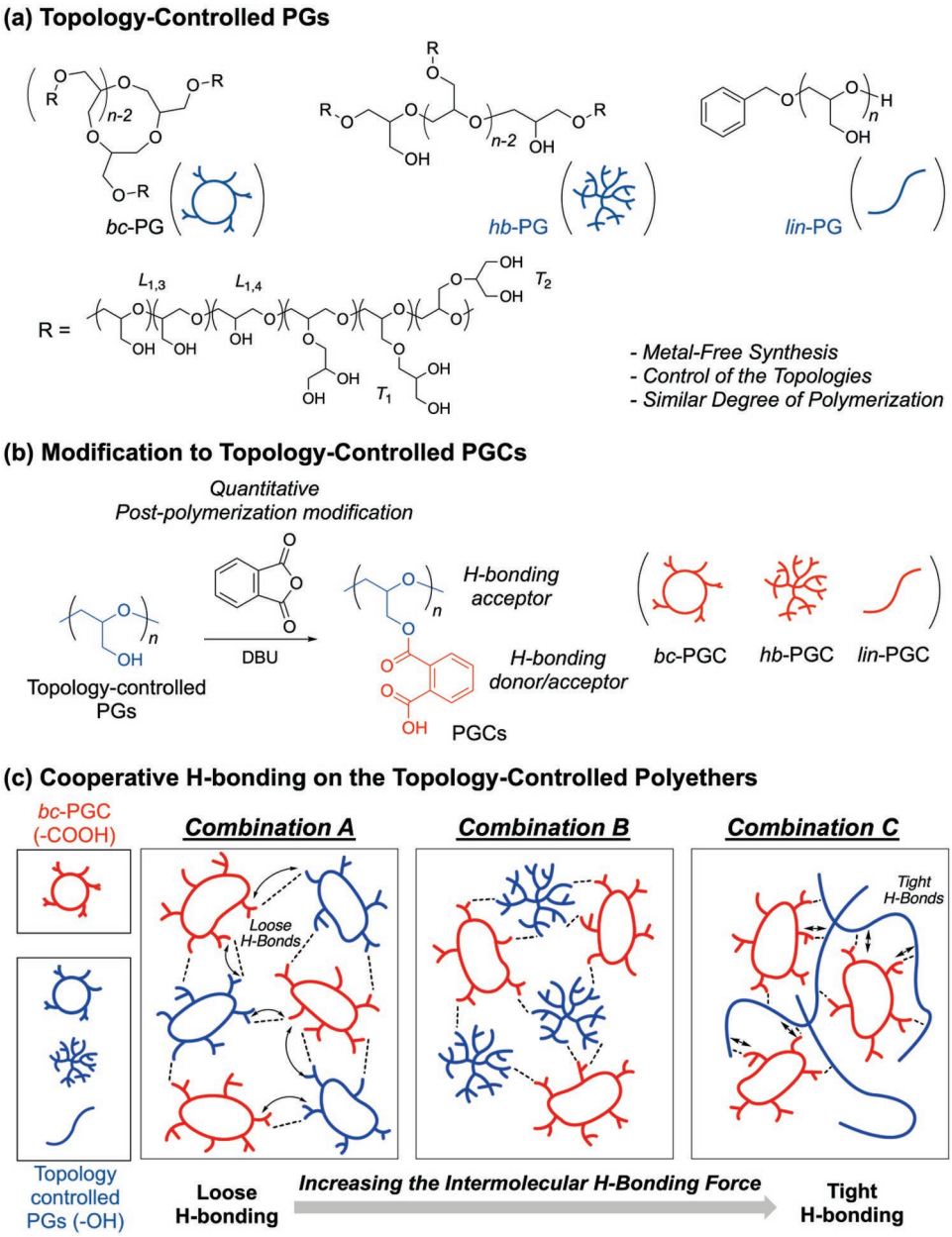

Scheme 1. a) Topology-controlled PGs used in this study; b) quantitative post-polymerization modification of topology-controlled PGs to form the corresponding PGCs; c) diagrams illustrating the cooperative H-bonding networks in the bulk state for each combination of *bc*-PGC with the topology-controlled PGs.

quantitatively introduced into the polymer backbone (Figure S9, Supporting Information).

2.3. of Topology-Dependent H-Bonding on the Physical Properties of PGC in the Bulk and Solution States

To study the effect of the topologies of the polymers on their bulk state properties, the three topology-controlled PGCs were synthesized with similar absolute molecular weights and subjected to thermal analysis by DSC (**Figure 2**). Here, the topology-controlled PGCs exhibit different T_g values, attributable to changes to the inter- and intramolecular H-bonding motifs of the polymers depending on their topology ($T_{g,bc\text{-PGC}}$ = 61 °C, $T_{g,hb\text{-PGC}}$ = 46 °C, and $T_{g,lin\text{-PGC}}$ = 33 °C). Interestingly, after introducing the aromatic carboxylic acids into the PG backbone, the T_g values clearly increase for all polymer topologies. Additionally, while *bc*-PG shows the lowest T_g value of the PG topologies, *bc*-PGCs exhibit the highest T_g value of the PGC topologies. These observations suggest that the degree of H-bonding between the polymer chains changes considerably after the introduction of the aromatic carboxylic acid groups.[28,32] Additionally, the ortho-positioned carboxylic acids may facilitate favorable intermolecular H-bonding interactions

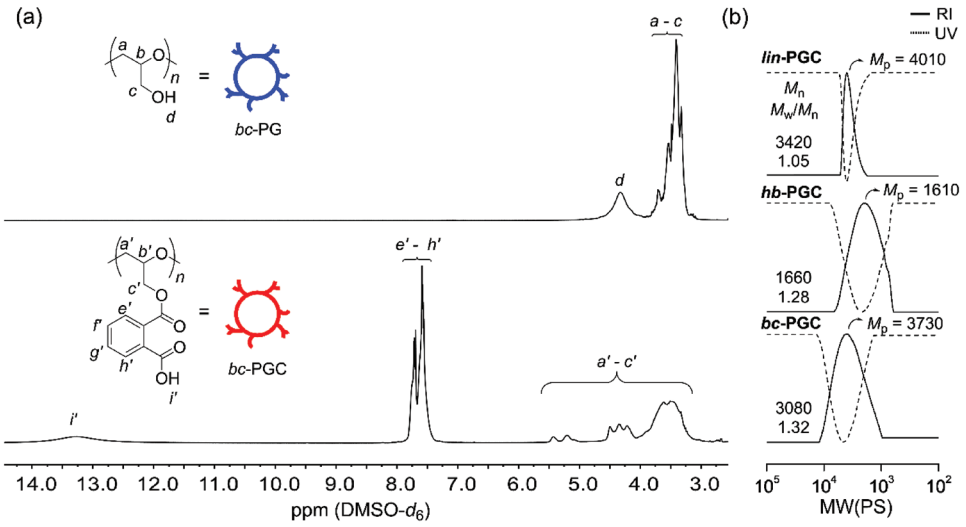

Figure 1. Structural analysis of the obtained topology-controlled polymers: a) 1H NMR spectra of *bc*-PG (top) and *bc*-PGC (bottom); b) RI and UV-SEC curves for the obtained topology-controlled PGCs.

between the polymer chains. *hb*-PGC exhibits an intermediate T_g value between those of the linear and branched cyclic topologies, as similarly observed for *hb*-PG, suggesting that a close correlation exists between the degrees of H-bonding and branching in the polymers.

Next, the properties of the topology-controlled PGCs in aqueous solution were studied. The *bc*-, *hb*-, and *lin*- PGCs retain negative charges in solution with zeta potentials of −39.8, −50.3, and −29.7 mV, respectively, at pH 7, resulting from the deprotonation of the carboxylic acid groups (Figure S10, Supporting Information). Additionally, when the degree of protonation is increased by the addition of 1.0 M HCl, the transmittance of the PGC solutions decreases sharply to 0% between pH 4 and 5 depending on the PGC topology (**Figure 3**). Considering that the pK_a of a typical polymeric carboxylic acid ranges between pH 4.7 and 5.0, this phenomenon may occur via intermolecular H-bond formation between the carboxylic acids and the oxygen atoms in the polyether backbone, as well as between the pendant group carboxylic groups of adjacent polymer chains to form dimers.[24,33]

As previously illustrated in Figure 1b, PGCs with different topologies and similar absolute molecular weights exhibit different relative molecular weights, indicating that the hydrodynamic diameter is dependent on the polymer topology ($M_{n,lin\text{-}PGC}$ = 3420, $Đ$ = 1.05; $M_{n,bc\text{-}PGC}$ = 3080, $Đ$ = 1.32; $M_{n,hb\text{-}PGC}$ = 1660, $Đ$ = 1.28).[28] In addition, interestingly, the pH response of the topology-controlled PGCs (as measured at 50% transmittance) depends on their hydrodynamic diameter (Figure 3). For example, the *lin*-PGC, which shows the largest hydrodynamic diameter, also exhibits the largest pH sensitivity compared to those of *hb*- and *bc*-PGCs. This is possible because the aromatic carboxylic acids with larger hydrodynamic diameters readily facilitate self-association through intermolecular H-bonding with other polymer chains, leading to the formation of larger polymer aggregates in the solution.

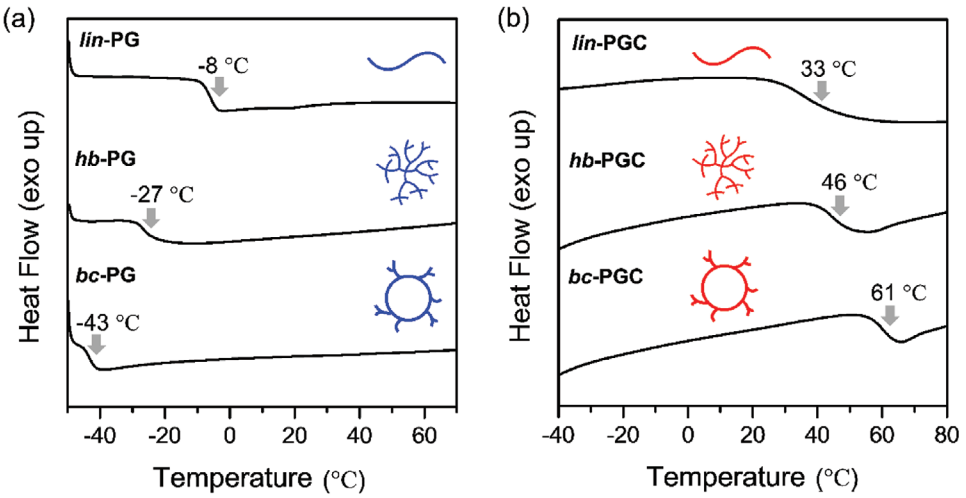

Figure 2. DSC thermograms of the topology-controlled a) PGs and b) PGCs. The 2nd heating scan is collected at a rate of 10°C min^{-1} after heating up to 80 °C.

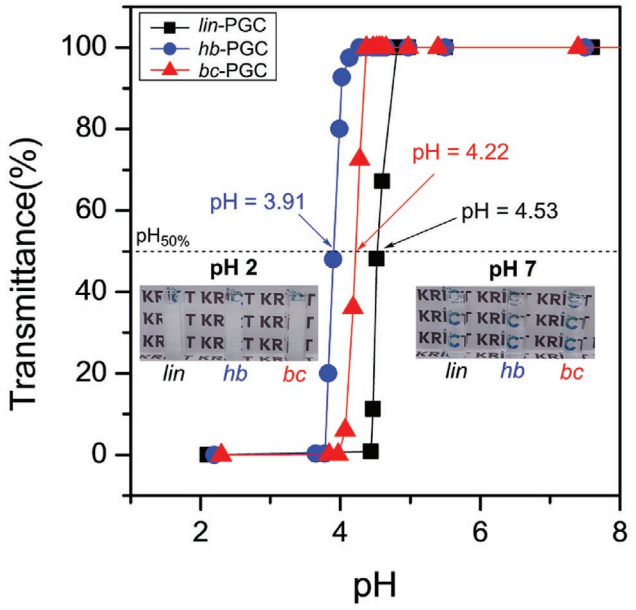

Figure 3. Transmittance change at 500 nm for the aqueous topology-controlled PGC solutions under varying pH conditions. The polymer concentration was fixed at 10 mg mL^{-1}. The inset optical images illustrate the change in transparency of the respective PGC solutions between pH 2 and 7.

2.4. Tunable Adhesive Properties of the Topology-Controlled PGCs via Cooperative H-Bonding

Next, we assessed the potential of the topology-controlled PGCs as adhesives based on their dynamic H-bonding interactions. In particular, lap shear tests were conducted to evaluate the effect of the polymer topology on the adhesive properties of PGC (**Figure 4**). To optimize the loading amount of *bc*-PGC for the adhesive strength tests, varying concentrations of *bc*-PGC in ethanol were used to obtain surface densities between 0.08 and 0.32 mg cm^{-2} on the glass substrates (Figure S11, Supporting Information). An optimal adhesion strength of 1.35 MPa was subsequently observed at a surface density of 0.16 mg cm^{-2}. While *bc*-PGC has a low degree of polymerization (DP = 37),[28] this value is similar to the adhesion strengths observed in our previous work on aliphatic carboxylic acid-derived polymers.[24] In addition, depending on the polymer topology, the adhesion strengths of the PGCs decrease to 1.16 and 0.94 MPa for *hb*- and *lin*-PGC, respectively (Figure 4b). This observation is in good agreement with the observed hierarchy of the T_g values for the topology-controlled PGCs ($T_{g,bc\text{-PGC}} > T_{g,hb\text{-PGC}} > T_{g,lin\text{-PGC}}$), suggesting that the adhesion strength also depends on the H-bonding motifs of the different topologies in the bulk state. The adhesive properties of *bc*-PGC were further examined with other substrates, including steel, PMMA, PC, and PTFE (Figure 4c). Notably, *bc*-PGC exhibits relatively lower adhesion performances on all other substrates compared to that on glass, thus indicating that H-bonding significantly influences the adhesion performance of this polymer.

Furthermore, we attempted to enhance the adhesion performance of *bc*-PGC by adding topology-controlled PGs as physical crosslinkers to facilitate cooperative H-bonding. Topology-controlled PGs have numerous pendant hydroxyl groups along the polymer chain, which can promote cooperative H-bonding with the carboxylic acid groups in *bc*-PGC depending on their polymer topologies. To optimize the mixing ratio of *bc*-PGC to the various PGs, a series of mixtures was evaluated with molar ratios of 2:1 and 1:1 for each topology on a glass substrate (Figure 4d; Figure S12, Supporting Information). At an equimolar mixing ratio, the adhesion performance of each mixture varies from 180% to 260% depending on the PG topology used, whereas the observed enhancement is relatively lower for the 2:1 mixing ratio. The combination of *bc*-PGC and *lin*-PG exhibits the highest adhesion performance; considering the observed T_g values associated with the preferred intermolecular H-bonding in each polymer topology, this combination may induce tighter H-bonding between the polymer chains, thus leading to the formation of an outstanding cooperative H-bonding network (Scheme 1c). The adhesion performance of this *bc*-PGC/*lin*-PG combination was further demonstrated by applying the adhesive mixture to a lat pull-down machine (Video S1, Supporting Information). Surprisingly, a lift-up of 30 kg was performed repetitively using two glass substrates connected by the *bc*-PGC/*lin*-PG adhesive. Furthermore, this polymer mixture exhibits remarkable enhancements in adhesion performance when applied to the other substrates (Figure 4e).

Finally, the biocompatibility of the topology-controlled PGCs was evaluated using MTT assays with animal fibroblast cells from subcutaneous connective tissue (cell line L929). Here, the *lin*-PGC showed relatively low cell viability compared to other PGCs, however, the *hb*-PGC and *bc*-PGC retained superior cellular viability ≈100% at concentrations up to 1 000 μg mL^{-1}, indicating the high potential of these polymer adhesives for biological and biomedical applications (Figure S13, Supporting Information).

3. Conclusions

In this study, the design and synthesis of topology-controlled aromatic carboxylic acid-derivatized polyethers were demonstrated to achieve robust cooperative H-bonding between polymer chains. Topology-controlled PGs, along with linear PGs as control samples, were prepared via the metal-free ring-opening polymerization of glycidol using frustrated Lewis pairs. Subsequently, aromatic carboxylic acid groups were successfully introduced into the topology-controlled PGs via a simple post-polymerization process utilizing DBU as a nucleophilic catalyst. The resulting polymer composition was examined using ^{1}H NMR, SEC, and TGA, which indicated that the modification method afforded an approximately quantitative conversion of the hydroxyl groups on the PG backbone for all the topologies studied. The resulting topologies of PGC (linear, hyperbranched, and branched cyclic), which possessed multiple H-bonding donor and acceptor moieties within a single repeating unit, exhibited different T_g values because of the change in the inter- and intramolecular H-bonding motifs depending on their unique structures. In particular, the branched cyclic-type polymer exhibited the largest increase in T_g after the introduction of the aromatic carboxylic acid groups into the PG backbone, indicating that intermolecular

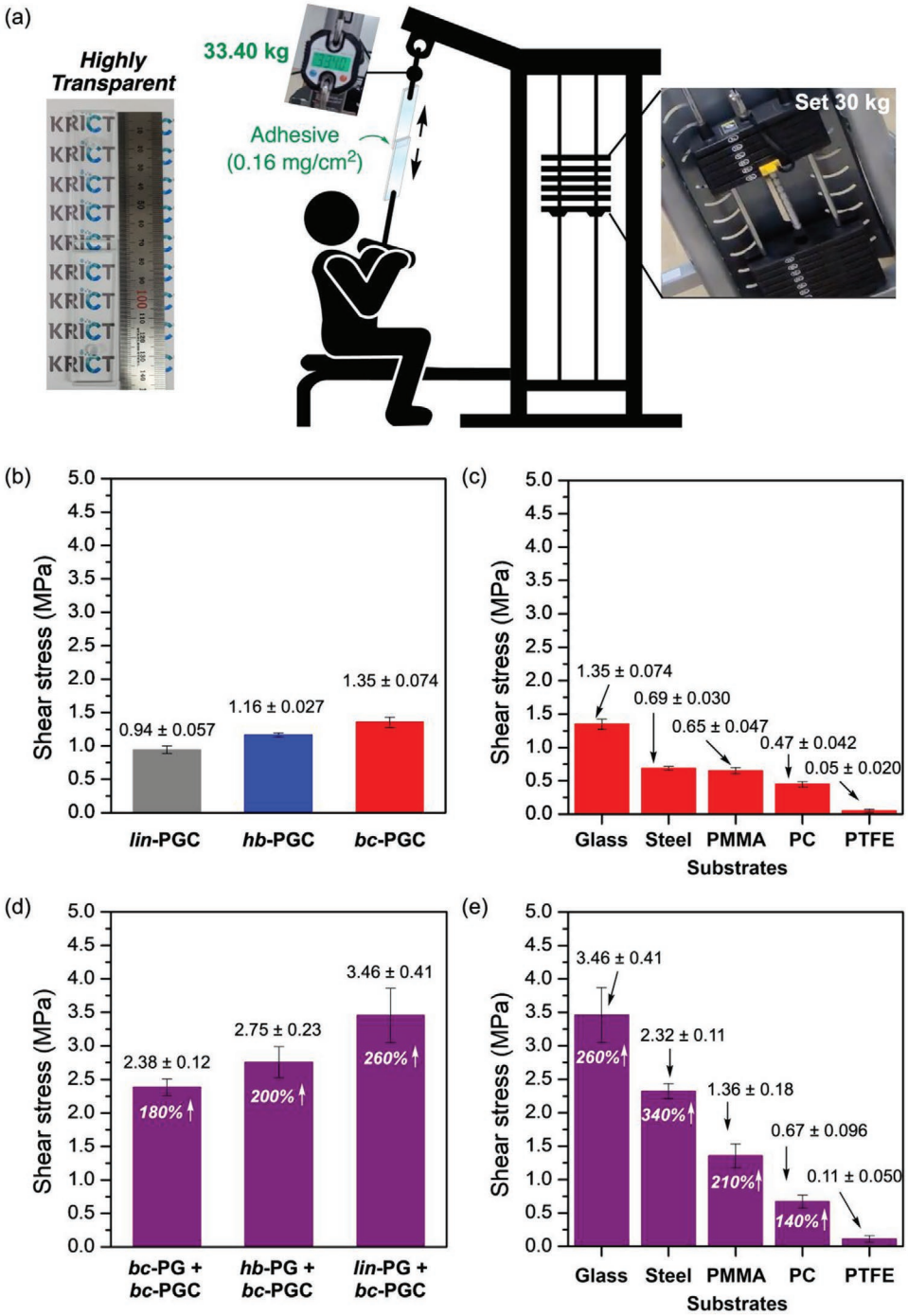

Figure 4. Lap shear adhesion testing of the topology-controlled PGCs: a) Optical image of the *bc*-PGC/*lin*-PG-coated glass substrate (left) and a schematic illustrating a lat pull-down of a 30 kg weight using the *bc*-PGC/*lin*-PG-coated glass substrate as a cable connector (right); b) observed shear stress of the topology-controlled PGCs on a glass substrate; c) observed shear stress of *bc*-PGC samples on various substrates; d) observed shear stress of *bc*-PGC mixed with various topologies of PG in a 1:1 molar ratio (the percentages in the bars indicate the increase in shear stress relative to *bc*-PGC only); e) observed shear stress of the 1:1 *bc*-PGC/*lin*-PG mixture on various substrates (1:1 molar ratio) (the percentages in the bars indicate the increase in shear stress relative to *bc*-PGC only on each substrate). All samples were loaded on the substrates with a surface density of 0.16 mg cm^{-2}.

H-bonding was considerably increased. The pH-dependent self-association properties of the PGCs in solution were also found to vary based on the polymer topology. Furthermore, a remarkable enhancement in adhesion performance via cooperative H-bonding between *bc*-PGC and topology-controlled PGs was demonstrated by lap shear tests on several substrates and a weight-lifting demonstration via a lat pull-down machine; here, a 1:1 *bc*-PGC/*lin*-PG combination produced the

largest increase in adhesion strength. All the synthesized PGCs also demonstrated excellent biocompatibility approaching 100% cell viability, as evaluated by the MTT assay. We, therefore, expect this new class of cooperative H-bonding between topology-controlled polymers to contribute to the development of advanced adhesives with considerable potential for biological and biomedical applications. A detailed characterization of the adhesive properties of topology-controlled PGCs in terms of different cooperative H-bonding motifs will be the subject of our future research.

4. Experimental Section

Materials: Tris(pentafluorophenyl)borane (BCF, Sigma-Aldrich; >95%), benzyl alcohol (Sigma-Aldrich; >99.8%), phosphazene base *t*-BuP_4 solution (0.8 M in hexane, Sigma-Aldrich), benzoic acid (Sigma-Aldrich; >99.5%), dimethyl sulfoxide (DMSO, Wako; 99%), *N*,*N*-dimethylformamide (DMF, Sigma-Aldrich; 99.8%), 1.8-diazabicyclo[5.4.0] undec-7-ene (DBU, Sigma-Aldrich; ≥99%), phthalic anhydride (Sigma-Aldrich; ≥99%), sodium hydroxide (Sigma-Aldrich; ≥98%), ethylene glycol (Sigma-Aldrich; ≥99%), hydrochloric acid (Sigma-Aldrich; ≥37%), acetonitrile (Wako; ≥99.9%), ethanol (Wako; ≥99.5%), and diethyl ether (Samchun Chemicals; 99%) were used as obtained from the manufacturers. Glycidol (GD, Sigma-Aldrich; >96%) and tetralin (Sigma-Aldrich; 99%), and tributylamine (Sigma-Aldrich; ≥98.5%) were dried overnight over calcium hydride and purified by distillation before use. Toluene (Sigma-Aldrich; ≥99.9%) was purified by passing it through purification columns (JCM, JCM-3SPS-SA-6) and bubbling with dry nitrogen gas for more than 15 min immediately before use. Deuterated dimethyl sulfoxide (DMSO-d_6, ≥99.9%) was purchased from Cambridge Isotope Laboratories, Inc.

Preparation of the Topology-Controlled PGs (Polyglycidols): *bc*-PG, *hb*-PG, and *lin*-PG were synthesized according to previously reported procedures.[27–29]

Synthesis of the Topology-Controlled PGCs via Post-Polymerization Modification with Phthalic Anhydride and DBU: Each topology-controlled PG (*bc*-PG, *hb*-PG, and *lin*-PG) (0.37 g, 5.0 mmol) was mixed with DBU (1.49 mL, 10.0 mmol) and acetonitrile (10 mL) in a 50 mL round-bottom flask. Phthalic anhydride (0.89 g, 6.0 mmol) was then added to the solution. Subsequently, the solution was stirred for 30 min at 25 °C, after which the mixture was quenched to pH 1 via the addition of 6 M HCl. The solvent was then removed by rotary evaporation, after which the crude mixture was diluted with ethyl acetate. The organic layer was then washed and extracted with water, followed by drying over Na_2SO_4. The solvent was then evaporated to obtain the modified PGCs (yield ≈80% for each PGCs).

Measurements: The M_n and M_w/M_n of polymers were measured by Size-exclusion chromatography at 40 °C using tetrahydrofuran (THF) as an eluent. For the THF-SEC, three polystyrene-gel columns [LF-404 (from Shodex); pore size, 150 Å; 8 mm i.d. × 300 mm, LF-404 (from Shodex); pore size, 500 Å; 8 mm i.d. × 300 mm, LF-404 (from Shodex); pore size, 1500 Å; 8 mm i.d. × 300 mm] were connected to a PU-4180 pump, a RI-4035 refractive-index detector, and a UV-4075 UV detector (JASCO) and the flow rate was set to 0.1 mL min^{-1}. The columns were calibrated against 8 standard polystyrene samples (Shodex; M_p = 1160–676000; M_w/M_n = 1.03–1.11) for obtained topology-controlled PGCs samples. ^{1}H nuclear magnetic resonance (NMR) spectra were recorded in ppm using an Ultrashield spectrometer (Bruker) operating at 300 MHz. All spectra were recorded in deuterated DMSO-d_6 at room temperature. Fourier transform infrared (FT-IR) spectra were recorded using a NOCOLET 6700 FT-IR spectrometer (Thermo Scientific) with an attenuated total reflection module. The thermal stabilities of the polymers were determined by thermogravimetric analysis (TGA) using a Q500 thermogravimetric analyzer (TA Instruments). All measurements were performed under a N_2 atmosphere between 25 and 800 °C at a heating rate of 10 °C min^{-1}. Differential scanning calorimetry (DSC) measurements were performed using a Q2000 calorimeter (TA Instruments). The polymer samples were measured under a dry nitrogen flow at a heating or cooling rate of 10 °C min^{-1}.

pH Response Tests of the Topology-Controlled PGCs: *bc*-PGC, *hb*-PGC, and *lin*-PGC were dispersed in deionized water at a concentration of 10 mg mL^{-1}, after which 1.0 M NaOH solution was added to induce polymer dissolution. Next, 1.0 M HCl was added dropwise to each solution while monitoring the transmittance change at 500 nm using a UV–vis spectrophotometer (V-770, JASCO).

Lap Shear Adhesion Tests: Each topology-controlled PGC was dissolved in ethanol (0.1 g mL^{-1}). A droplet of the PGC solution was then deposited on a glass, polytetrafluoroethylene (PTFE), poly(methyl methacrylate) (PMMA), polycarbonate (PC), or stainless-steel substrate (25 × 5 mm^2). Before each test, the specimen was immobilized with a binder clip and dried in a vacuum oven at over 15 °C higher than the glass transition temperature (T_g) of each sample for 12 h and cooled to room temperature. The adhesion tests were then performed on a universal testing machine (UTM, LF-Plus, Lloyd Instruments) at a velocity of 1.3 mm min^{-1} and 25 °C. The results were obtained by calculating the average values and the standard deviation of three replicates.

In Vitro Cell Viability Assay: To evaluate the cellular toxicity of the topology-controlled PGCs, a 3-(4,5-dimethylthiazol-2-yl)-2,5-diphenyltetrazolium bromide (MTT) assay was performed. L929 cells were grown in RPMI 1640 media containing 10% fetal bovine serum and 1% penicillin–streptomycin (10 000 U mL^{-1}) and cultured in Heracell™ 150i at 37 °C with 5% CO_2. Thereafter, the cells were seeded in a 96-well plate at a concentration of 5×10^4 cells mL^{-1} and incubated until fulfilled the plate. Topology-controlled PGC solutions of different concentrations (0.1, 1, 10, 100, 500, and 1 000 μg mL^{-1} in cell media) were added to the cell cultures, after which the cells were incubated in the dark for an additional 24 h at 37 °C with 5% CO_2. MTT (10 μL, 5 mg mL^{-1} PBS, pH 7.4) was then added to each well, followed by further incubation for 4 h. Subsequently, DMSO was added to dissolve the resulting formazan crystals, and their absorbance was recorded at 490 nm using a Victor X5 multilabel plate reader (Perkin Elmer). To perform the experiments on human subjects, rules or permissions from the relevant institutional authorities are not in place in the country where the experiments were performed. All procedures performed in studies involving human participants were in accordance with the ethical standards of the national committee and with the 1964 Helsinki Declaration and its later research amendments or comparable ethical standards. In addition, informed consent was obtained from all individual participants involved in the study.

Supporting Information

Supporting Information is available from the Wiley Online Library or from the author.

Acknowledgements

This study was supported by the Ministry of Trade, Industry and Energy (MOTIE, Korea) under the Industrial Technology Innovation Program (no. 20011123) and the Korea Research Institute of Chemical Technology (KRICT) (no. KS2341-20). This work was supported by the National Research Foundation of Korea (NRF-2021R1A2C3004978).

Conflict of Interest

The authors declare no conflict of interest.

Author Contributions

The manuscript was written with contributions from all authors. All the authors approved the final version of the manuscript.

Data Availability Statement

The data that support the findings of this study are available on request from the corresponding author. The data are not publicly available due to privacy or ethical restrictions.

Keywords

cooperative H-bonding, poly(glycidoxy carbonyl benzoic acid), polyethers, polymer adhesives, polymer topology control

Received: February 22, 2023
Revised: April 10, 2023
Published online:

[1] K. Matyjaszewski, N. V. Tsarevsky, *J. Am. Chem. Soc.* **2014**, *136*, 6513.
[2] S. E. Seo, C. J. Hawker, *Macromolecules* **2020**, *53*, 3257.
[3] R. A. Shenoi, J. K. Narayanannair, J. L. Hamilton, B. F. Lai, S. Horte, R. K. Kainthan, J. P. Varghese, K. G. Rajeev, M. Manoharan, J. N. Kizhakkedathu, *J. Am. Chem. Soc.* **2012**, *134*, 14945.
[4] B. I. Voit, A. Lederer, *Chem. Rev.* **2009**, *109*, 5924.
[5] D. A. Tomalia, H. Baker, J. Dewald, M. Hall, G. Kallos, S. Martin, J. Roeck, J. Ryder, P. Smith, *Dendritic Macromolecules: Synthesis of Starburst Dendrimers Macromolecules* **1986**, *19*, 2466.
[6] C. J. Hawker, J. M. J. Frechet, *J. Am. Chem. Soc.* **1990**, *112*, 7638.
[7] X. Feng, D. Taton, E. Ibarboure, E. L. Chaikof, Y. Gnanou, *J. Am. Chem. Soc.* **2008**, *130*, 11662.
[8] S. Y. Lee, M. Kim, T. K. Won, S. H. Back, Y. Hong, B.-S. Kim, D. J. Ahn, *Nat. Commun.* **2022**, *13*, 6532.
[9] J. Ochs, C. A. Pagnacco, F. Barroso-Bujans, *Prog. Polym. Sci.* **2022**, *134*, 101606.
[10] L. Gao, J. Oh, Y. Tu, T. Chang, C. Y. Li, *Polymer* **2019**, *170*, 198.
[11] M. D. Hossain, J. C. Reid, D. Lu, Z. Jia, D. J. Searles, M. J. Monteiro, *Biomacromolecules* **2018**, *19*, 616.
[12] L. J. Prins, D. N. Reinhoudt, P. Timmerman, *Angew. Chem., Int. Ed.* **2001**, *40*, 2382.
[13] J. D. Watson, F. H. Crick, *Molecular Structure of Nucleic Acids* **1953**, *171*, 737.
[14] D. Eisenberg, *Proc. Natl. Acad. Sci. USA* **2003**, *100*, 11207.
[15] A. H. Hofman, I. A. van Hees, J. Yang, M. Kamperman, *Adv. Mater.* **2018**, *30*, 1704640.
[16] J. Jin, P. Hassanzadeh, G. Perotto, W. Sun, M. A. Brenckle, D. Kaplan, F. G. Omenetto, M. Rolandi, *Adv. Mater.* **2013**, *25*, 4482.
[17] J. Wang, D. Zhang, F. Chu, *Adv. Mater.* **2020**, *33*, 2001135.
[18] G. Qing, Q. Lu, X. Li, J. Liu, M. Ye, X. Liang, T. Sun, *Nat. Commun.* **2017**, *8*, 461.
[19] G. M. Ter Huurne, I. K. Voets, A. R. A. Palmans, E. W. Meijer, *Macromolecules* **2018**, *51*, 8853.
[20] P. Song, H. Wang, *Adv. Mater.* **2019**, *32*, 1901244.
[21] S. J. D. Lugger, S. J. A. Houben, Y. Foelen, M. G. Debije, A. P. H. J. Schenning, D. J. Mulder, *Chem. Rev.* **2022**, *122*, 4946.
[22] J. J. B. van der Tol, G. Vantomme, A. R. A. Palmans, E. W. Meijer, *Macromolecules* **2022**, *55*, 6820.
[23] M. A. R. Meier, *Macromol. Rapid Commun.* **2019**, *40*, 1800524.
[24] G. Kwon, M. Kim, W. H. Jung, S. Park, T.-T. H. Tam, S.-H. Oh, S.-H. Choi, D. J. Ahn, S.-H. Lee, B.-S. Kim, *Macromolecules* **2021**, *54*, 8478.
[25] M. G. Mazzotta, A. A. Putnam, M. A. North, J. J. Wilker, *J. Am. Chem. Soc.* **2020**, *142*, 4762.
[26] S.-H. Hwang, H. Kim, H. Ryu, I. E. Serdiuk, D. Lee, T.-L. Choi, *J. Am. Chem. Soc.* **2022**, *144*, 1778.
[27] S. E. Kim, H. J. Yang, S. Choi, E. Hwang, M. Kim, H.-J. Paik, J.-E. Jeong, Y. I. Park, J. C. Kim, B.-S. Kim, S.-H. Lee, *Green Chem.* **2022**, *24*, 251.
[28] S. E. Kim, Y.-R. Lee, M. Kim, E. Seo, H.-J. Paik, J. C. Kim, J.-E. Jeong, Y. I. Park, B.-S. Kim, S.-H. Lee, *Polym. Chem.* **2022**, *13*, 1243.
[29] J. Song, L. Palanikumar, Y. Choi, I. Kim, T.-Y. Heo, E. Ahn, S.-H. Choi, E. Lee, Y. Shibasaki, J.-H. Ryu, B.-S. Kim, *Polym. Chem.* **2017**, *8*, 7119.
[30] W.-C. Shieh, S. Dell, O. Repic, *J. Org. Chem.* **2002**, *67*, 2188.
[31] K. E. Price, C. Larrivée-Aboussafy, B. M. Lillie, R. W. McLaughlin, J. Mustakis, K. W. Hettenbach, J. M. Hawkins, R. Vaidyanathan, *Org. Lett.* **2009**, *11*, 2003.
[32] C. Schubert, M. Schömer, M. Steube, S. Decker, C. Friedrich, H. Frey, *Macromol. Chem. Phys.* **2017**, *219*, 1700376.
[33] A. S. Michaels, O. Morelos, *Ind Eng Chem* **1955**, *47*, 1801.